

# Formation and Growth of Intermetallics at the Interface Between Lead-free Solders and Copper Substrates

T.A. Siewert  
NIST  
Boulder, Colorado

J.C. Madeni and S. Liu  
Colorado School of Mines  
Golden, Colorado

## Abstract

Intermetallic formation and growth were studied for the alloys Sn-3.2Ag-0.8Cu, Sn-3.5Ag, Sn-0.7Cu, and Sn-9Zn. Coupons of solder joints (prepared by melting some of each solder alloy on a copper-plated circuit board) were subjected to thermal aging tests for 20, 100, 200, and 500 hours at 70, 100, and 150 °C. Also, the activation energies for the formation of each intermetallic compound and the total intermetallic layer for the four copper-solder systems were determined. The results confirm that the formation of intermetallic layers is controlled by diffusion and that the intermetallic layers grow by thermal activation in a parabolic manner. The total thickness of the intermetallic compounds produced at 150 °C for 500 hours and the activation energies for the total intermetallic layer in the four copper-solder systems were: 14 μm and 0.74 eV/atom for Cu/Sn-3.2Ag-0.8Cu, 13 μm and 0.85 eV per atom for Cu/Sn-3.5Ag, 14 μm and 0.68 eV/atom for Cu/Sn-0.7Cu, and 19 μm and 0.35 eV/atom for Cu/Sn-9Zn.

## Key Words

copper; intermetallics; lead-free solders; silver; solder; tin

## Introduction

Lead-free solder alloys cannot be simply substituted for conventional lead-containing alloys because of differences in their mechanical and physical properties. To use the new lead-free alloys in reliable and enduring products, accurate data must be inserted into the finite-element models of board designs. This is an attempt to develop some of the needed data for the intermetallics that form between four of these solders and the copper pads.

We decided to compare four of the lead-free solders that have been shown to be promising in studies by the National Center for Manufacturing Sciences (NCMS), and by the National Electronics Manufacturing Initiative (NEMI) [1-2]. These were the alloys Sn-3.2Ag-0.8Cu, Sn-3.5Ag, Sn-0.7Cu, and Sn-9Zn.

The formation of intermetallic phases in an electronic joint is usually disadvantageous because the intermetallic phases are typically brittle and may be more susceptible to crack growth. However, the intermetallic compounds are an indication of chemical bonding at the substrate/solder interface [3], so small amounts of intermetallic compounds can be

considered to indicate that the soldering process has formed a good bond. In some cases, small amounts of intermetallic compounds can even produce some improvements in the mechanical and thermal properties of solder joints, and promote wetting and bonding processes [4]. According to Harris [5], the presence of the intermetallics Ag<sub>3</sub>Sn and Cu<sub>6</sub>Sn<sub>5</sub> in the tin solid solution in the alloys Sn-3.5Ag and Sn-0.7Cu respectively, improves hardness and resistance to fatigue. However, the negative effects tend to dominate. Their hardness is usually several times greater than that of either the copper or the tin, and their resistivity is usually many times greater than that of the copper. In any case, it is almost impossible to avoid the formation of intermetallics, so their presence (and their properties) must be factored into designs.

The intermetallic phases are products of the solder-substrate interactions. An initial layer forms during the soldering process, and continues to grow in the solid state, especially at elevated temperatures. The growth of the intermetallic layer follows a parabolic growth curve, as expressed by equation (1):

$$X = (kt)^{1/2}, \quad (1)$$

where  $X$  is the thickness of the intermetallic layer,  $t$  is the time, and  $k$  is the growth constant at a specific temperature.

This mechanism assumes that the growth of the intermetallic compound layer is controlled by bulk diffusion of reactants to the reaction interface. The parabolic reduction in growth rate with time reflects the increase in the diffusion path as the already formed intermetallic layers impede the transport of additional reactants. In some cases, multiple intermetallics, such as both  $\text{Cu}_3\text{Sn}$  and  $\text{Cu}_6\text{Sn}_5$ , can form between copper and tin.

### Procedures

The solder alloys were deposited on coupons cut from an FR4 PCB, which had been plated with about 45 or 50  $\mu\text{m}$  of copper. The coupons were about 25 mm square. After a protective coating was removed from the copper surface, the coupons were cleaned by rinsing with ethanol, then a water-based solution of ammonium hydroxide, trisodium phosphate, and sodium tetraborate pentahydrate. After the copper surfaces dried (a few seconds), a solution of water-based phosphoric acid was applied (for the silver and copper bearing alloys). Next, the three molten solders, at 50 °C above their melting temperatures, were deposited on the substrates and the coupons were cooled in air to ambient temperature. In the case of alloy Sn-9Zn, the copper surface was prepared by use of commercial zinc chloride- and ammonium chloride-based paste. The cleaning agent was applied on the copper surface right before the molten solder alloy was deposited on it, and provided better wetting than the phosphoric acid solution chosen for the other three solder alloys.

The copper/solder coupons were thermally aged using a furnace that was accurate and uniform to within  $\pm 1$  °C. To avoid oxidation during thermal aging, industrial-grade argon gas was fed to the furnace. The specimens were aged according to a 3 by 4 matrix design (temperatures 70, 100 and 150 °C, for 20, 100, 200 and 500 hours). The furnace was open only for a short time (< 2 seconds) as the specimens were extracted, which had an insignificant effect on the temperature. The specimens were water-quenched as they were removed from the furnace.

After thermal aging, the specimens were cut in half, perpendicular to the flat surface of the copper substrate, and cold mounted in epoxy to display the cross-section for metallographic analysis. Using standard metallographic techniques, the mounted specimens were ground and polished down to a 0.5  $\mu\text{m}$  diamond slurry, followed by vibratory polishing for 40 minutes in an aqueous solution of colloidal silica. The final finish was quite satisfactory for resolving the intermetallic compounds at the copper/solder interface. The copper/solder interfaces of the specimens were examined by use of light microscopy to differentiate the intermetallic layers, scanning electron microscopy (SEM) to obtain

backscattered electron images (BEI) that contrasted the chemical composition differences between different phases, and energy dispersive spectroscopy (EDS) for element identification. Quantitative measurements of the thickness of the intermetallic layers were made using a digital image analysis system. To obtain an accurate average thickness for the very uneven interfaces, between 20 and 40 measurements were taken at the interface on each specimen. The intermetallic compounds (IMCs) were identified using EDS. After centering the electron beam on the area of interest, the spectrum was acquired and an approximate composition was calculated.

### Results and Discussion

A typical copper-solder interface, after soldering but before thermal aging, is shown in Figure 1. The most noticeable features of the structure (from bottom to top) are the circuit-board substrate, the copper pad, and the solder. Only at high magnifications can very small amounts of  $\text{Cu}_6\text{Sn}_5$  be resolved at the copper/solder interface [6]. Note that the copper/solder interface is not perfectly planar. In fact, the copper boundary has a very irregular shape.

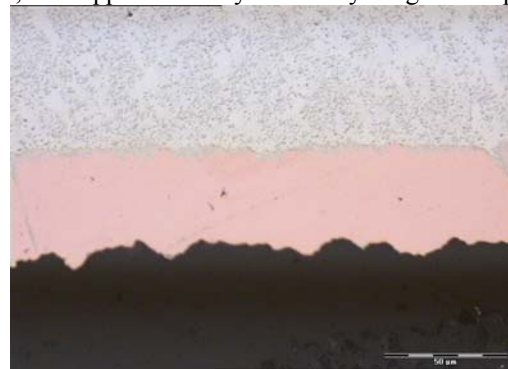


Figure 1. Copper/Sn-3.5Ag solder interface prior to thermal aging.

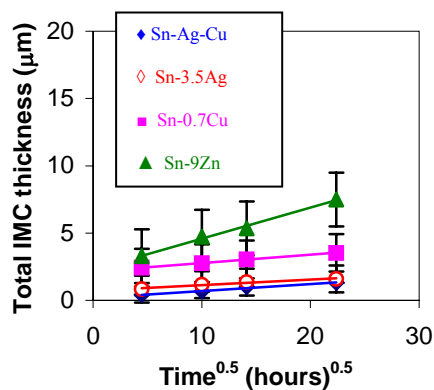
The thermal aging changed the microstructure at the copper/solder interface as the intermetallic layers grew. After only 20 hours, a very thin dark line of  $\text{Cu}_6\text{Sn}_5$  was visible at the copper/Sn-3.5Ag interface, even at this relatively low magnification of 600 X. As the aging time increased, the IMC layer grew, but more slowly. The specimens exposed for 100, 200, and 500 hours display two distinct intermetallic layers,  $\text{Cu}_3\text{Sn}$  and  $\text{Cu}_6\text{Sn}_5$ . A similar trend is observed in the other systems ( $\text{Cu}/\text{Sn}-3.2\text{Ag}-0.8\text{Cu}$ ,  $\text{Cu}/\text{Sn}-0.7\text{Ag}$  and  $\text{Cu}/\text{Sn}-9\text{Zn}$ ). However, in the case of the  $\text{Cu}/\text{Sn}-9\text{Zn}$  interface, only one intermetallic phase is observed,  $\text{Cu}_5\text{Zn}_8$ . The thickness of the layers of these intermetallic compounds varied with the solder system.

Thermodynamic calculations predict the formation of  $\text{Cu}_5\text{Zn}_8$  in the Sn-9Zn alloy, instead of the  $\text{Cu}_3\text{Sn}$  and  $\text{Cu}_5\text{Sn}_6$  intermetallic compounds usually found in tin-

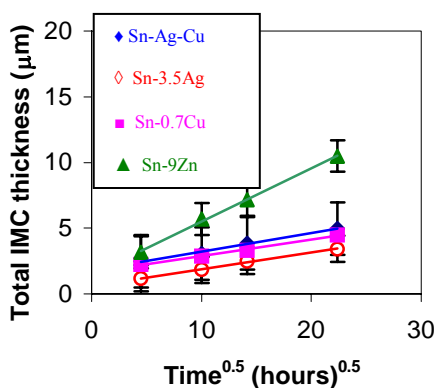
rich alloys. The free energy change of the reactions ( $-7.8$  kJ/mol for  $\text{Cu}_3\text{Sn}$ ,  $-7.4$  kJ/mol for  $\text{Cu}_5\text{Sn}_6$  and  $-12.3$  kJ/mol for  $\text{Cu}_5\text{Zn}_8$ ) calculated using the Gibbs-Helmholtz equation, clearly indicate that  $\text{Cu}_5\text{Zn}_8$  is the most likely to form.

The kinetics of the IMC growth was determined as a function of aging time and temperature for both individual  $\text{Cu}_3\text{Sn}$  and  $\text{Cu}_6\text{Sn}_5$  layers and the combined ( $\text{Cu}_3\text{Sn} + \text{Cu}_6\text{Sn}_5$ ) IMC thicknesses. The mean values of the total intermetallic layer thicknesses at the greatest growth condition,  $150^\circ\text{C}$  for 500 hours, in the four copper-solder systems were found to be:  $13\text{ }\mu\text{m}$  for  $\text{Cu}/\text{Sn-3.5Ag}$ ,  $14\text{ }\mu\text{m}$  for  $\text{Cu}/\text{Sn-3.2Ag-0.8Cu}$ ,  $14\text{ }\mu\text{m}$  for  $\text{Cu}/\text{Sn-0.7Cu}$ , and  $19\text{ }\mu\text{m}$  for the  $\text{Cu}/\text{Sn-9Zn}$  alloy.

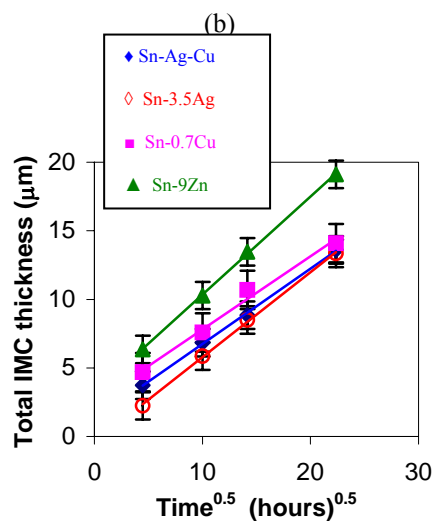
The observed total IMC thickness and time relationships at  $70$ ,  $100$  and  $150^\circ\text{C}$ , are shown in Figures 2 (a), (b), and (c). They all obey the predicted parabolic relationship. The slopes of the lines in Figure 2 indicate the rate of IMC growth. As expected, as the temperature increased, the rate of IMC layer growth increased. At all three temperatures, the intermetallic in  $\text{Sn-9Zn}$  grows distinctly faster than that of the others alloys, which are fairly tightly grouped. At  $70$  and  $100^\circ\text{C}$ , the intermetallic in  $\text{Sn-3.5Ag}$  grows at a slightly slower rate, while at  $150^\circ\text{C}$ , the intermetallic in  $\text{Sn-3.2Ag-0.8Cu}$  grows at the slowest rate.



(a)



(b)



(c)

Figure 2. Total IMC growth ( $\text{Cu}_3\text{Sn} + \text{Cu}_6\text{Sn}_5$ ) at the copper/solder interface at three temperatures, (a)  $70^\circ\text{C}$ , (b)  $100^\circ\text{C}$ , and (c)  $150^\circ\text{C}$ . In each case, the bars show the range in thickness measurements (from between 20 and 40 individual measurements for each specimen), and the symbol is at the mean.

Similar analyses were done with the individual IMCs in each copper/solder system. The general observation is that their growth also obeys the parabolic relation, as in the case of the growth of the total IMC. The following observations on the individual layers are based on analysis of the mean values, but some of the scatter bands are fairly wide (as shown by the vertical bars), compared to the differences between the means, so some of these trends are weak.

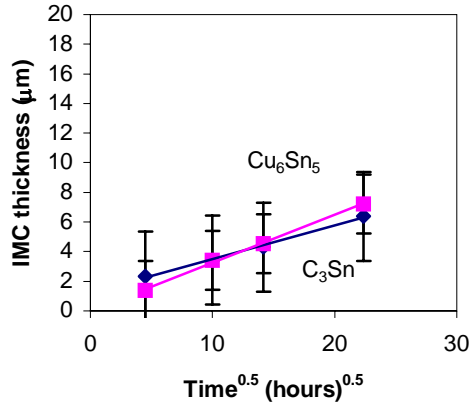
In the case of the  $\text{Cu}/\text{Sn-3.2Ag-0.8Cu}$  joint system, shown in Figure 3 (a), the initial thicknesses and the growth rates for the two intermetallics are very similar. From the slight difference in the slopes of the means, we might conclude that the  $\text{Cu}_6\text{Sn}_5$  intermetallic grows at a slightly faster rate than the  $\text{Cu}_3\text{Sn}$ .

For the  $\text{Cu}/\text{Sn-3.5Ag}$  system, shown in Figure 3 (b), one sees that the  $\text{Cu}_6\text{Sn}_5$  and  $\text{Cu}_3\text{Sn}$  layers start at almost the same thickness. By 150 hours, the thickness of  $\text{Cu}_3\text{Sn}$  is distinctly less, so its growth rate is slower. Perhaps this difference in behavior from that of the previous alloy is due to a larger fraction of tin is reacting with silver to form  $\text{Ag}_3\text{Sn}$  at the  $\text{Cu}_6\text{Sn}_5$  growth front.

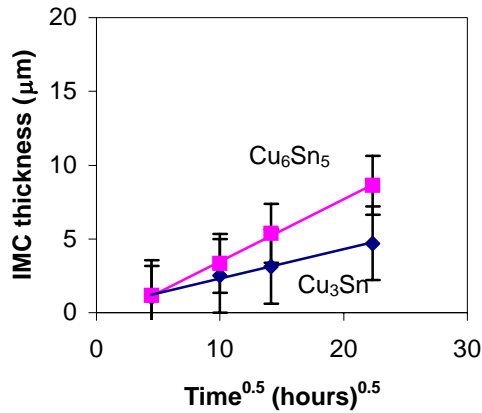
In the case of the  $\text{Cu}/\text{Sn-0.7Cu}$  system, shown in Figure 3 (c),  $\text{Cu}_3\text{Sn}$  starts with a thicker layer, but grows at approximately the same rate as  $\text{Cu}_6\text{Sn}_5$ . The  $\text{Cu}_3\text{Sn}$  layer may grow faster here than for the previous two alloys because no  $\text{Ag}_3\text{Sn}$  is formed in

this system, so more tin atoms can migrate through the  $\text{Cu}_6\text{Sn}_5$  layer to form  $\text{Cu}_3\text{Sn}$ .

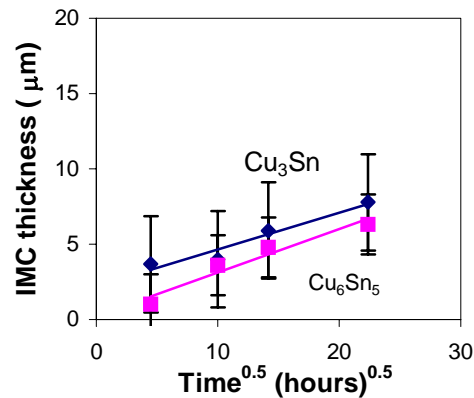
In the case of the Cu/Sn-9Zn system, only  $\text{Cu}_5\text{Zn}_8$  forms. Figure 3 (d) shows its growth is faster than for the sum of both of the intermetallics in the other alloys.



(a)



(b)



(c)

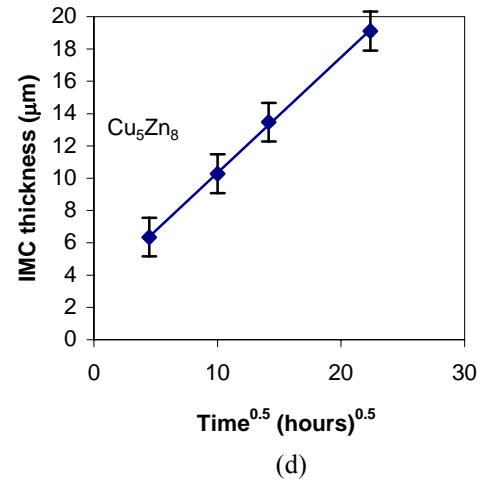


Figure 3. Individual intermetallic component layers growth for specimens aged at 150 °C, (a) Sn-3.2Ag-0.8Cu, (b) Sn-3.5Ag, (c) Sn-0.7Cu, and (d) Sn-9Zn. In the first three plots,  $\text{Cu}_3\text{Sn}$  is identified by the diamonds and  $\text{Cu}_6\text{Sn}_5$  by the squares.

The constant  $k$  in equation (1) is determined from the slopes of the lines in the IMC thickness as a function of log time plots. After adding the temperature dependency and normalizing the equation to a linear form using a regression model, the log  $k$  can be determined as a function of  $(1/T)$  plots for the individual phases and for the total IMC. Figures 4 through 7 display these plots for each alloy system. The constant  $k_0$  is expressed in units of [microns\*hour<sup>-1/2</sup>], with the gas constant,  $R$ , equal to 8,314 J/(mole\*K), implying that the temperature must be in Kelvin. Using these units, the activation energy,  $Q$ , is determined in units of J/mol. The activation energy,  $Q$ , is calculated from the slope ( $s = -Q/2.3R$ ) of the log  $k$  versus  $1/T$  plots.

Both Figures 4 (a) and (b) are for the Cu/Sn-3.2Ag-0.8Cu system. The slopes of the lines in Figure 4 (a) suggest similar activation energies for the two intermetallic compounds. Since the slope of the line in Figure 4 (b) is almost the same as those of the individual IMCs, the activation energy for the total IMC will be very close to those of the individual IMCs.

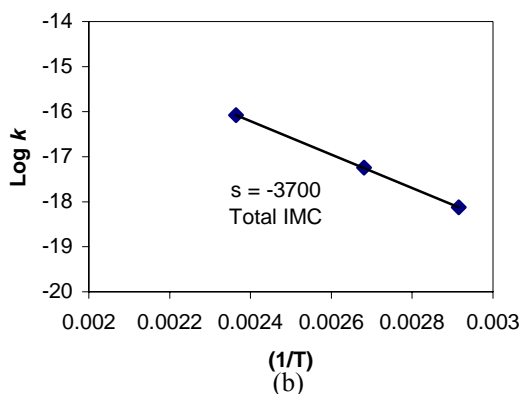
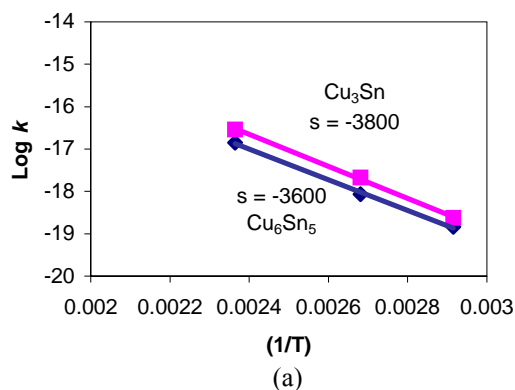


Figure 4. Log  $k$  as a function of  $(1/T)$  for (a) individual IMCs ( $\text{Cu}_3\text{Sn}$  and  $\text{Cu}_6\text{Sn}_5$ ), (b) total IMC ( $\text{Cu}_3\text{Sn} + \text{Cu}_6\text{Sn}_5$ ) in the Cu/Sn-3.2Ag-0.8Cu system. In Figure 4 (a), the squares represent the  $\text{Cu}_3\text{Sn}$  data.

The plots in Figures 5 (a) and (b) are for the Cu/Sn-3.5Ag system. The slopes of the lines in Figure 5 (a) suggest a higher activation energy for the  $\text{Cu}_6\text{Sn}_5$  formation than for  $\text{Cu}_3\text{Sn}$ . The line on Figure 5 (b) corresponds to the combination of the two intermetallic phases in one layer. As expected, its slope suggests an intermediate value for the activation energy.

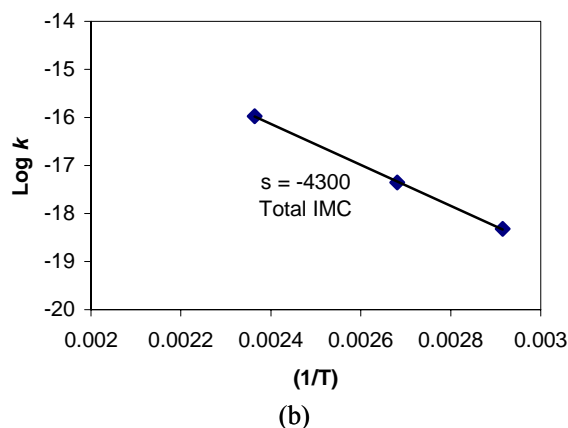
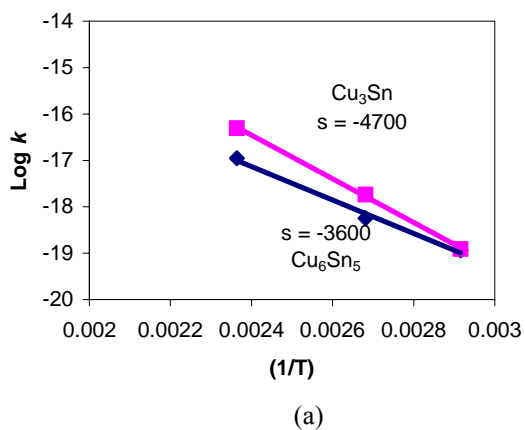


Figure 5. Log  $k$  as a function of  $(1/T)$  for (a) individual IMCs ( $\text{Cu}_3\text{Sn}$  and  $\text{Cu}_6\text{Sn}_5$ ), (b) total IMC ( $\text{Cu}_3\text{Sn} + \text{Cu}_6\text{Sn}_5$ ) in the Cu/Sn-3.5Ag system. In Figure 5 (a), the squares represent the  $\text{Cu}_3\text{Sn}$  data.

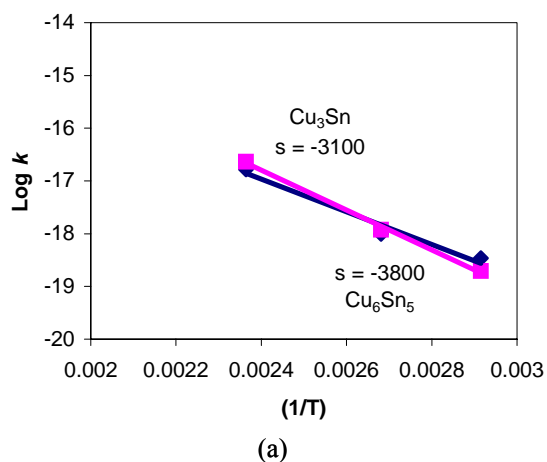


Figure 6. Log  $k$  as a function of  $(1/T)$  for (a) individual IMCs ( $\text{Cu}_3\text{Sn}$  and  $\text{Cu}_6\text{Sn}_5$ ), (b) total IMC ( $\text{Cu}_3\text{Sn} + \text{Cu}_6\text{Sn}_5$ ) in the Cu/Sn-0.7Cu system. In Figure 6 (a), the squares represent the  $\text{Cu}_3\text{Sn}$  data.

The plots for the Cu/Sn-0.7Cu system are exhibited in Figures 6 (a) and (b). The slope of the  $\text{Cu}_6\text{Sn}_5$  line indicates an activation energy higher than that of the  $\text{Cu}_3\text{Sn}$ . The intersection of the two lines in Figure 6 (a) indicates that at high temperatures the rate of formation of  $\text{Cu}_6\text{Sn}_5$  is higher than that of  $\text{Cu}_3\text{Sn}$ ; at low temperatures the opposite occurs. The slope of the line on Figure 6 (b), which is for the total IMC thickness ( $\text{Cu}_3\text{Sn} + \text{Cu}_6\text{Sn}_5$ ), indicates an intermediate value for the activation energy.

In the case of the Cu/Sn-9Zn system, a single activation energy is determined. Since the slope of the line in Figure 7 is the smallest among the four copper/solder systems, the smallest value of activation energy is observed.

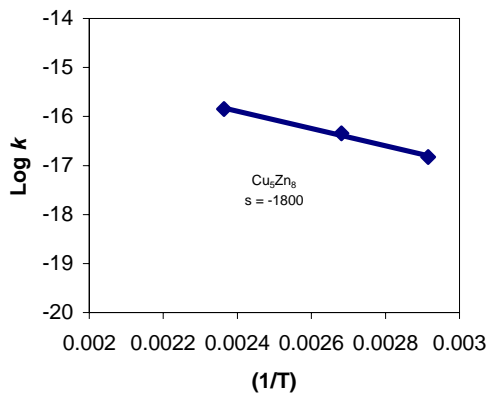


Figure 7. Log k as a function of (1/T) for the total IMC in the Cu/Sn-9Zn system (in this system there is only one IMC).

As the activation energy of a specific intermetallic compound increases, the formation and growth of this compound becomes more difficult. On the other hand, low activation energies indicate easier formation and growth of IMCs. The calculated activation energies represent both the formation and motion of vacancies responsible for the interfacial reaction. Q, the activation energy, is stated in the following equation:

$$Q = \Delta H_m + \Delta H_f, \quad (2)$$

where  $\Delta H_f$  is the enthalpy change needed to form a mole of vacancies and  $\Delta H_m$  is the enthalpy change or energy barrier that must be overcome to move a mole of atoms into vacancies.

The activation energies for the total IMC thickness and for the individual phases for the four solder alloys are presented in Table 1. The activation energy data for the Cu/Sn-3.5Ag and Cu/Sn-0.7Cu joint systems are in good agreement with previous studies found in the literature [7, 8]. In the case of the Cu/Sn-

3.2Ag-0.8Cu and Cu/Sn-9Zn joint systems, no comparison data were found.

Table 1. Activation energies, Q, derived from the data for the total and individual IMCs in the Cu/Sn-3.2Ag-0.8Cu, Cu/Sn-3.5Ag, Cu/Sn-0.7Cu, and Cu/Sn-9Zn joint systems.

ALLOY	IMC	Q (kJ/mol)	Q (eV/atom)
Sn-3.2Ag-0.8Cu	Total	70	0.74
	$\text{Cu}_3\text{Sn}$	69	0.72
	$\text{Cu}_6\text{Sn}_5$	72	0.75
Sn-3.5Ag	Total	82	0.85
	$\text{Cu}_3\text{Sn}$	69	0.72
	$\text{Cu}_6\text{Sn}_5$	90	0.93
Sn-0.7Cu	Total	66	0.68
	$\text{Cu}_3\text{Sn}$	59	0.61
	$\text{Cu}_6\text{Sn}_5$	72	0.75
Sn-9Zn	$\text{Cu}_5\text{Zn}_8$	34	0.35

## Conclusions

- Three intermetallic compounds were found at the Cu/Sn-3.5Ag and Cu/Sn-3.2Ag-0.8Cu interfaces:  $\text{Cu}_3\text{Sn}$ ,  $\text{Cu}_6\text{Sn}_5$  and  $\text{Ag}_3\text{Sn}$ .
- At the Cu/Sn-0.7Cu interface, two IMC layers were found:  $\text{Cu}_3\text{Sn}$  and  $\text{Cu}_6\text{Sn}_5$ .
- At the Cu/Sn-9Zn interface, only  $\text{Cu}_5\text{Zn}_8$  was found.
- The intermetallic layers grow by thermal activation in a parabolic manner.
- The IMCs,  $\text{Cu}_3\text{Sn}$ ,  $\text{Cu}_6\text{Sn}_5$  and  $\text{Cu}_5\text{Zn}_8$ , formed layers of uneven thickness and grew at different rates, depending on the alloy composition.
- From the sole standpoint of IMC growth, Sn-3.5Ag seems to be the best solder material for electronic soldering because the IMC at the Cu/Sn-3.5Ag interface grows more slower than in the other three systems.
- The solder alloy Sn-9Zn had the fastest IMC growth.
- The other two alloys, Sn-3.2Ag-0.8Cu and Sn-0.7Cu, had growth rates that were intermediate, but close to that of Sn-3.5Ag.

## References

1. National Center for Manufacturing Sciences (NCMS), "The Lead-free Solder Project", NCMS Report 0401RE96, (1997)
2. "Roadmap of Lead-Free Assembly in North America," JISSO/PROTEC Forum 2002, November 19-20, 2002; Japan.
3. Shan-Pu Yu, Moo-Chin Wan, Min-Hsiung Hon, "Formation of Intermetallic Compounds at Eutectic Sn-Zn-Al Solder/Cu

Interface", J. Mater. Res., Vol. 16, No. 1, Jan (2001).

4. Y. G. Lee, J. G. Duh, "Characterizing the Formation and Growth of Intermetallic Compounds in the Solder Joint", Journal of Material Science, 33, (1998), pp. 5569-5572.
5. Paul G. Harris, Kaldev S. Chaggar, "The Role of Intermetallic Compounds in Lead-free Soldering" Soldering and Surface Mount Technology, 10/3, (1998), pp. 38-52.
6. A. Zibri, A. Clark, L. Zavalij, P. Borgesen, and E. J. Cotts, "The Growth of Intermetallic Compounds at Sn-Ag-Cu Solder/Cu and Sn-Ag-Cu/Ni Interfaces and the Associated Evolution of the Solder Microstructure", JOM, Vol. 30, No. 6, (2001), pp. 1157-1164.
7. P. T. Vianco, A. C. Kilgo, R. Grant, "Intermetallic Compound Layer Growth Kinetics in Non Lead Bearing Solders", Sandia National Laboratories, Albuquerque, NM, (1995).
8. D. R. Flanders, E. G. Jacobs and R. F. Pinizzotto, "Activation Energies of Intermetallic Growth of Sn-Ag Eutectic Solder on Copper Substrates", JOM, Vol. 26, No. 7, (1997).